Spectroscopy of Exotic Baryons with CLAS: Search for Ground and First Excited States

M. Battaglieri (co-spokesperson, contact person),
R. De Vita (co-spokesperson), M. Anghinolfi, M.M. Giannini,
M. Osipenko, G. Ricco, M. Ripani, E. Santopinto, M. Taiuti,
Istituto Nazionale di Fisica Nucleare and Università di Genova

V. Kubarovsky (co-spokesperson), J. Cummings, P. Stoler,
Rensselaer Polytechnic Institute and JLab

V. Burkert, L. Guo, D. Weygand,
Jefferson Lab

J. Price, B. Nefkens,
University of California at Los Angeles

E. Pasyuk,
Arizona State University

R. Schumacher,
Carnegie Mellon University

P. Eugenio, A. Ostrovidov,
Florida State University

I. Strakovsky,
George Washington University

M. Holtrop,
University of New Hampshire

M. Khandaker, C. Salgado
Norfolk State University

D. Carman, K. Hicks,
Ohio University

C. Djalali, R. Gothe, D. Tedeschi, M. Wood,
University of South Carolina

and the CLAS collaboration

Abstract

The existence of baryon states beyond the minimal qqq configuration is one of the open questions of strong interaction physics. While such states are not prohibited by QCD, no experimental evidence had ever been found until recently. The first evidence of a narrow resonance with $S = +1$, named Θ^+, was reported by the LEPS Collaboration. This result was then confirmed by other experimental groups, including the CLAS Collaboration who found a signal in the reactions $\gamma D \to pK^+K^-(n)$ and $\gamma p \to \pi^+K^-K^+(n)$. However, due to the limited statistics, the reported results are not yet conclusive and experiments with higher statistics are needed to confirm these findings and do extensive checks of the systematic dependencies.

In this proposal we request 25 days of beam time with CLAS and the Hall-B Bremsstrahlung photon tagger to run a photoproduction experiment on a proton target. Using a 4 GeV electron beam energy and a 40 cm liquid hydrogen target cell, we will be able to increase the existing statistics by more than a factor of 10, measuring simultaneously two production channels, $\gamma p \to \bar{K}^0\Theta^+$ and $\gamma p \to \pi^+K^-\Theta^+$, as well as two decay modes of the Θ^+, K^+n and K^0p. Our primary goal is to establish a firm and consistent phenomenology of the Θ^+ spectra, to determine in which production and decay channels the Θ^+ is seen, and what the production mechanisms are. This measurement will provide a solid foundation for a long-term plan for the investigation of the pentaquark spectrum and properties.

Contents

1 Introduction **4**

2 Theoretical Predictions **5**
2.1 Pentaquark quantum numbers and spectroscopy 6
2.2 Production mechanisms: total and differential cross sections 8

3 Previous pentaquark searches **10**

4 Present CLAS measurements **11**
4.1 Low-energy analysis 11
4.2 High-energy analysis 14
4.2.1 The reaction $\gamma p \to \bar{K}^0 K^+(n)$ 14
4.2.2 The reaction $\gamma p \to \pi^+ K^- \Theta^+$ 15

5 Experimental setup and proposed measurement **16**
5.1 Kinematics and Monte Carlo simulations: choice of magnetic field and energy range 16
5.2 New Start Counter 18
5.3 Running conditions 19
5.4 Statistical accuracy 20
5.5 Systematic errors 21

6 Summary **22**

A Appendix: Rate estimates **23**
A.1 Tagger rate 23
A.2 CLAS, Start Counter, and Trigger Rates 23
A.3 Trigger Logic and Accidental Rates 24
A.4 Trigger Efficiency 25

1 Introduction

The discovery of baryon states beyond the usual qqq configuration is of fundamental importance for the understanding of hadronic structure. QCD does not prohibit the existence of states with different configurations, as for example $qqqq\bar{q}$. In fact, measurements of nucleon structure functions from high energy lepton-nucleon experiments have shown for example that "sea" quarks ($q\bar{q}$ pairs) contribute significantly to the total momentum and the total spin of the nucleon. This has shown that the usual baryons are in fact an admixture of the standard qqq configuration and of $qqqq\bar{q}$, $qqqg$, ... In the past, experimental searches focussed on the search for pentaquark states, i.e. baryons with a minimal $qqqq\bar{q}$ structure where the $\bar{q}$ has a different flavor than the other quarks. These investigations did not provide any clear evidence, leading to the conclusion that discoveries in this field would not be possible in the short term [1]. As a consequence, this particular experimental program was abandoned and no further data analysis was pursued for many years. However, the lack of experimental proof left an open question about the physical manifestation of low-energy QCD.

In spite of the lack of clear evidence for the existence of such exotics, theoretical interest in this field has continued [2, 3, 4, 5, 6]. More recently, Diakonov et al. [7] made definite predictions about the masses and widths of a decuplet of pentaquark states (the so-called "antidecuplet"). The most intriguing aspect of such a multiplet is the presence of three states with exotic quantum numbers: the Θ^+ with $S = +1$, and the Ξ^{--} and Ξ^+ with $S = -2$. In particular the Θ^+ strangeness, never observed in the baryon sector and not compatible with a qqq state, requires a minimal pentaquark configuration of the type $uudd\bar{s}$. The widths of the exotic pentaquarks were predicted by this model to be very narrow ($\sim$10–15 MeV) implying that if such states exist they should be directly visible in the measured invariant masses without need for more sophisticated Partial Wave Analysis. These predictions triggered new experimental searches and led to the discovery of a Θ^+ candidate reported in October 2002 by the LEPS Collaboration [8]. Several other experimental groups followed [9, 10, 11, 12, 13, 14, 15], reporting evidence of a peak in the mass range 1525–1556 MeV, while first evidence of the Ξ^{--} was reported by the CERN experiment NA49 [16].

Many experiments are being analyzed for further evidence of pentaquark states. We present preliminary evidence that there may be <u>two</u> peaks in the missing mass spectra for $\gamma p \to \bar{K}^0\Theta^+$. After a series of cuts to reduce background and enhance the signal, we found evidence for a low-mass ($\sim$1526 MeV) and a high-mass ($\sim$1572 MeV) peak in both decay modes $\Theta^+ \to K^+n$ and $\Theta^+ \to K^0p$. Although this analysis is still in a preliminary stage, it may be the first observation of a pentaquark excited state with S=+1. Clearly, the discovery of a second state besides the widely reported Θ^+ would have very important implications for our understanding of pentaquark physics and would call for a broader program in exotic baryon spectroscopy.

With this proposal, we intend to begin a systematic study of the pentaquark spectrum, extending the existing measurements on proton targets. We will measure two production channels, $\gamma p \to \bar{K}^0\Theta^+$ and $\gamma p \to K^*\Theta^+$, as well as two decay modes of the Θ^+, K^+n and

$K^0 p$. With this dedicated run we hope to answer the following questions:
- are the present signals a statistical fluctuation?
- in which production and decay channels does the Θ^+ show up?
- what is the angular dependence of the associated K meson?
- what are the production mechanisms in terms of hadron dynamics?
- what are the relative production cross-sections and branching ratios?
and, most importantly,
-what are the masses and widths of pentaquarks produced in photoproduction and decaying to a K-nucleon final state?

This measurement is complementary to the "g2c" experiment approved by the last PAC; that experiment seeks to confirm exclusive production of a Θ^+ in $\gamma D \to pK^+K^-n$ final states.

This paper is organized as follows. In Section 2 we will discuss some of the recent theoretical predictions for pentaquark properties and production. In Sections 3 and 4 we will review the recent experimental results with particular care to the CLAS results. Finally, in section 5 we will describe the experimental setup and expected accuracy for the proposed experiment.

2 Theoretical Predictions

The recent experimental findings have renewed the interest in pentaquark phenomenology and have triggered a rapid increase in theoretical activity. One of the outcomes is the recent workshop on this topic at Jefferson Lab [17], while dedicated sessions have been or are being planned for other international conferences. Since the original Spring8 result was reported, more than 80 theoretical papers have appeared on the preprint servers, giving a clear demonstration of the relevance of this topic.

Theoretical predictions on the existence and properties of pentaquark baryons are based on a variety of models that treat the basic degrees of freedom quite differently. Due to the lack of a well-established phenomenology, at present different approaches result in different expectations for masses, widths, and quantum numbers of the Θ^+ and its companions. The result of the proposed experiment will help in constraining the model predictions.

In the next sections we will review some of the recent theoretical works with particular attention to the aspects related to this proposal: quantum numbers, excitation spectrum of the pentaquark, and production mechanisms (i.e. total and differential cross sections).

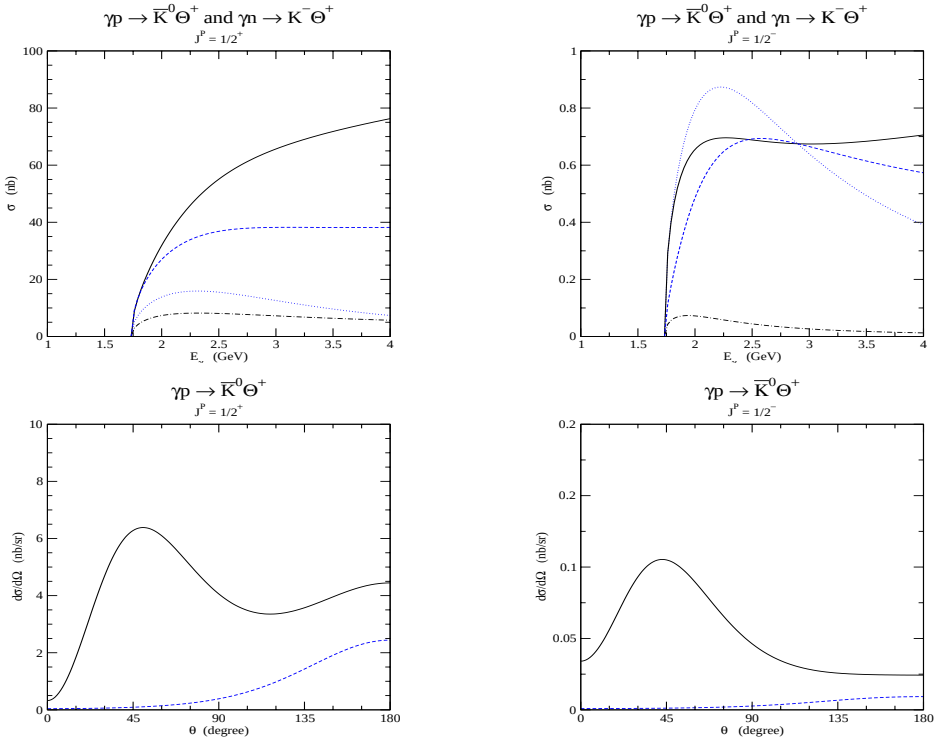

Figure 1: Total (top) and differential (bottom) cross sections for the reaction $\gamma N \to \bar{K}\Theta^+$. The left and right columns correspond to positive and negative Θ^+ parity. The solid and dot-dashed lines show the $\gamma p \to \bar{K}^0\Theta^+$ cross section for $g_{K^*N\Theta} = g_{KN\Theta}$ and with $g_{K^*N\Theta} = 0$. The dashed and dotted lines show the $\gamma n \to K^-\Theta^+$ cross section under the same assumptions. Note that the vertical scale of the right column is expanded compared with the left.

2.1 Pentaquark quantum numbers and spectroscopy

In the framework of the chiral soliton model, Diakonov and collaborators predicted [7] an anti-decuplet of pentaquarks in which the lowest mass state is the Θ^+ with I=0, spin-parity $1/2^+$, and mass of 1530 MeV. The predicted width is around 10–15 MeV, much narrower than what was expected based on previous calculations. The same quantum numbers are predicted in clustered quark models: a diquark-diquark-antiquark model was proposed by Jaffe and Wilczek [18], while Karliner and Lipkin [19] used the hypothesis of a diquark-triquark systems, each one being a color non-singlet. In this approach, the narrow width comes from the re-coupling of the color and flavor-spin of the clusters onto the color-singlet nucleon and kaon. In a constituent quark model approach, Capstick, Page and Roberts [20] related the narrow width to a possible I=2 and negative parity state that would have a isospin-violating strong decay. The same parity has been predicted by lattice QCD calculations [21] and QCD sum rules [22].

From the experimental point of view, the predictions of Θ^+ spin and parity may be tested relying on some minimal model assumptions. Limiting the spin to 1/2 or 3/2 and assuming that the produced Θ^+ is polarized, the different parity and populations of spin projection states will be reflected in the decay angular distribution. For instance, a kaon predominantly emitted at backward angles suggests a u-channel exchange mechanism, where the proton first dissociates into a Θ^+ and a kaon, then the Θ^+ absorbs the

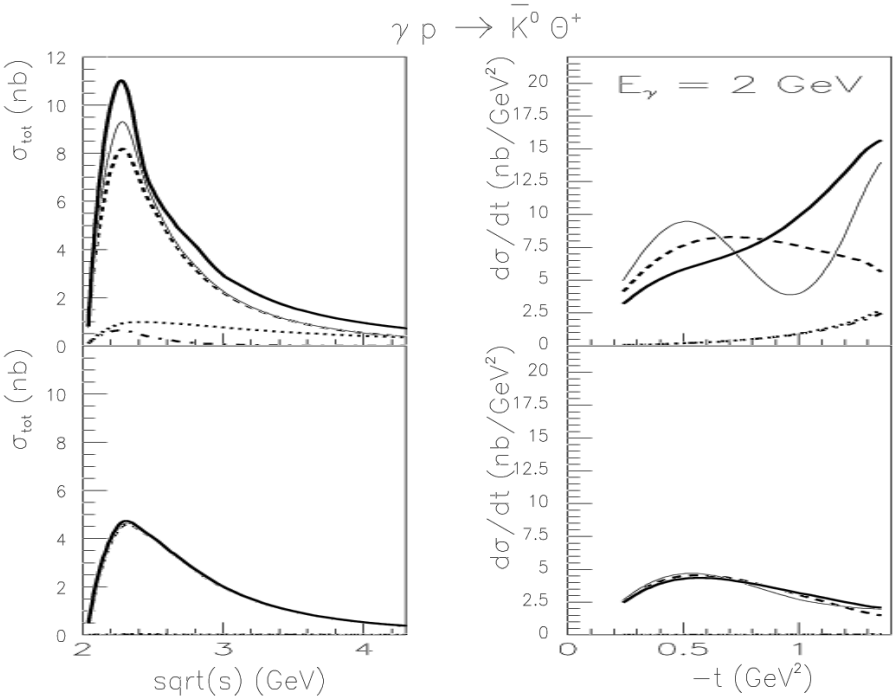

Figure 2: Regge model predictions for the $\gamma p \to \bar{K}^0\Theta^+$ reaction for Θ^+ positive parity (top) and negative parity (bottom). The left and right columns show the total and the differential cross section. Dashed: K^* Regge exchange; dashed-dotted: gauge-invariant $(s+u)$ channel exchange; thin solid: sum of K^* and $(s+u)$ Reggeized exchange; dotted: $(s+u)$ pole exchange; thick-dotted: sum of K^* and $(s+u)$ pole exchange.

photon. In this case, one can easily see that a spin-1/2 Θ^+ will be equally populated in spin projections by the absorption of the photon, while a spin 3/2 state will have different probabilities for populating $\pm 1/2$ and $\pm 3/2$ states by photon absorption, resulting in a non-uniform decay angular probability. This argument can be made more model-independent if events with very backward $\bar{K}^0$ angles are selected. In this case, one can make a collinear approximation where all incoming, outgoing, and intermediate particles are moving along the same direction. Therefore, by knowing the production mechanism and measuring the decay angular distribution, it may be possible to infer the spin value.

Theoretical efforts were also addressed to predict the pentaquark spectrum. A discussion of different scenarios for pentaquark spectroscopy is found in the paper by Close [23], where it is remarked that a spin-3/2 partner of the Θ^+ may exist. The predicted mass gap varies from 50 MeV, obtained in the Skyrme-soliton model by Borisuyk and collaborators [24], to 250 MeV, reported in Ref. [25]. Very recently, a general classification of all the possible pentaquark states based on symmetry considerations has been reported in [26]. From this model-independent discussion, it emerges that there should be a pair of states with spin 1/2 and 3/2, respectively, with a splitting due to a spin-orbit interaction

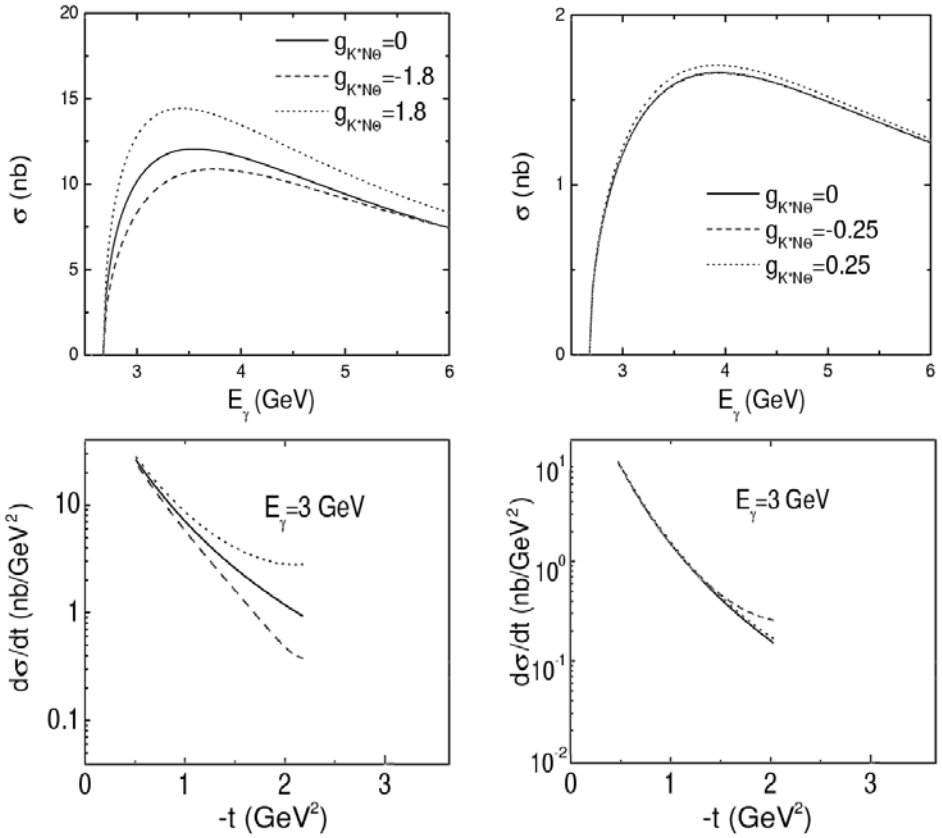

Figure 3: Total and differential cross section for reaction $\gamma p \to \pi^+ K^- \Theta^+$ for positive parity (left) and negative parity (right). The different curves corresponds to $g_{K^*N\Theta} = 1.8$ (dotted curves), 0 (solid curves), and -1.8 (dashed curves).

in the positive parity case, or to a spin-spin interaction in the negative parity case. The ground state is expected to have I=0 while the first excited should be an iso-triplet.

2.2 Production mechanisms: total and differential cross sections

Estimates of the total and differential cross sections for the reactions $\gamma p \to \bar{K}^0 \Theta^+$ have been carried out in hadronic models with effective Lagrangians [27, 28, 29, 30] and in the Regge theory approach [31]. At present, the production mechanisms are completely unknown and the available calculations include contributions from meson-exchange in the t-channel, baryon exchange in the s-channel, and pentaquark exchange in the u-channel. Varying the unknown coupling constants within reasonable ranges, such models are able to predict the total and differential cross sections according to different hypotheses for the Θ^+ quantum numbers (parity, spin, isospin, etc.).

Predictions for the total and differential cross sections for $\gamma p \to \bar{K}^0 \Theta^+$ from Ref. [30] and [31] are shown in Figs. 1 and 2. Both approaches show that, for a given Θ^+ parity, the angular distribution and the total cross section strongly depend on the inclusion of the K^* exchange in the t-channel. When this contribution is added, the differential cross section shows a peak at forward K^0 angles, and the total cross section increases by almost

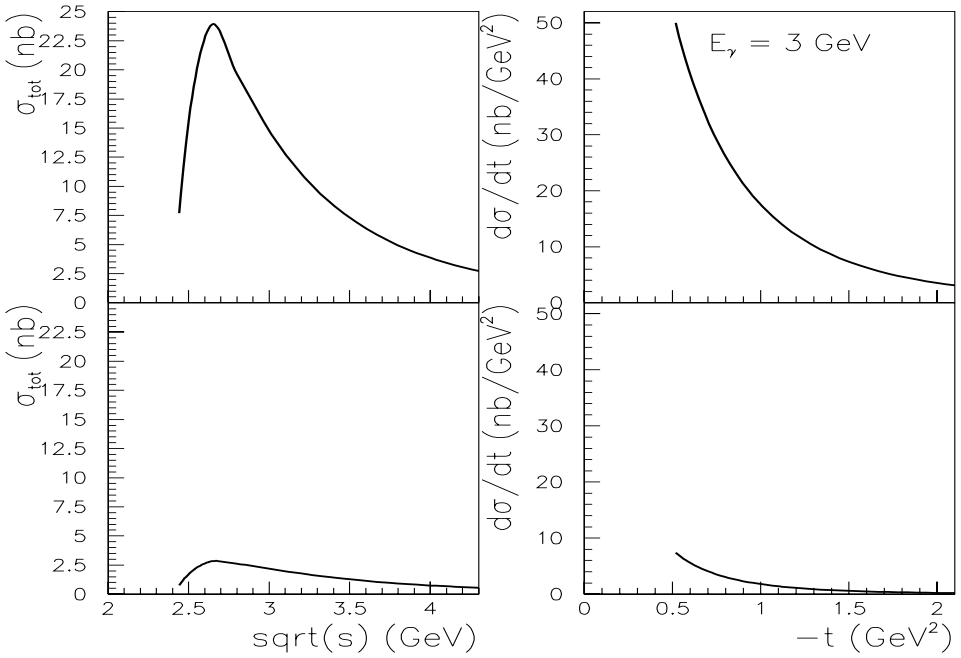

Figure 4: Regge model predictions for the $\gamma p \to \bar{K}_0^* \Theta^+$ reaction for both possible parities of the Θ^+. Upper panels: positive parity; lower panels: negative parity.

an order of magnitude. The coupling constant $g_{K^*N\Theta}$ is in fact unknown and the available theoretical estimates indicate that it may be anomalously small [32]. The measurement of the differential cross section in the whole angular range will help to determine the relevance of such a contribution, as well as the other production mechanisms. The predictions of the two models differ significantly in the energy behavior of the total cross section. In the Regge approach, it shows a steep fall-off with increasing photon energy, suggesting that the cross section peaks close to the production threshold. On the contrary, the effective Lagrangian approach predicts a smooth energy behavior. The measurement of the total cross section from the threshold to 3–4 GeV will allow us to test these different model predictions.

It is important to note that both calculations predict up to an order of magnitude difference in the cross section for positive and negative parity of the Θ^+. Thus, the measurement of the absolute cross section will help to determine the Θ^+ parity.

Similar calculations have been performed for the $\gamma p \to K^* \Theta^+$ [31] and $\gamma p \to K^- \pi^+ \Theta^+$ channels [33]. The differential cross section is, in both theories, predicted to peak at small momentum transfer t due to meson exchange dominance. In the calculation of Ref. [33], this feature remains even when the K^* exchange is suppressed due to the contribution of charged meson exchange, and the cross section estimate is less sensitive to the unknown coupling constants. The total cross section shows a behavior similar to that described for the $\gamma p \to \bar{K}^0 \Theta^+$ channel (see Figs. 3 and 4).

In addition, since the model calculations for $\gamma p \to \bar{K}^0 \Theta^+$ and $\gamma p \to K^* \Theta^+$ are based on the same parameters, the measurement of the differential and total cross sections for both channels will give strong constraints for the development of such theories.

3 Previous pentaquark searches

For many years, pentaquark searches used K^+-nucleon scattering and phase shift analyses. No conclusive evidence was found for the existence of resonances in this channel and the section on Pentaquarks was finally removed from the Particle Data Group after 1986. At that time the experimental search was focussed on masses of the order of 1.55-2.65 GeV and widths of the order of 100 MeV were expected. On the contrary, the present experimental indications are of a narrow state, with an intrinsic full width of less than 10 MeV. Such a narrow state may have escaped detection in the phase shift analyses due to the relatively large energy steps required by the limited statistics. Recent considerations of the kaon-nucleon data [34] have shown that a narrow state with a width not beyond a few MeV may be accommodated in the amplitude analysis, and that assuming (I)(J)(P)=(0)(1/2)(+) the χ^2 of the fit is improved. This analysis also pointed out that the available data show a gap around the 1540 MeV region, which prevents the fits from having a sizeable sensitivity to the Θ^+ and its parameters. This point clearly indicates that there is no obvious contradiction between the recent experimental evidence for a Θ^+ state and the previous body of scattering data.

As already mentioned, the first evidence of the Θ^+ was obtained in the photoproduction measurement performed by the LEPS Collaboration [8]. The signal was found in the reaction $\gamma n \to K^-\Theta^+ \to K^-K^+n$. The target was a CH_2 scintillator located just downstream of the primary hydrogen (LH_2) target. The signal was seen in the missing mass spectrum of the K^-, after cutting out sources of background from ϕ and $\Lambda(1520)$ production. Corrections to compensate for the neutron's Fermi motion in the carbon nucleus were applied. The final peak was found at a mass of 1540 ± 10 MeV, with a width less than 25 MeV, and a gaussian significance of 4.6 σ.

This result was shortly thereafter confirmed by the CLAS Collaboration who analyzed existing data on deuteron target looking at the channel $\gamma d \to K^-K^+np$. Events with the K^-K^+p in the final state were selected and the missing mass technique was used to identify the neutron. A peak was observed in the nK^+ invariant mass at a value of 1542 ± 5 MeV, with a width less than 21 MeV, and a statistical significance of more than 5 σ. Evidence of a Θ^+ candidate was also found in the reaction $\gamma p \to K^-\pi^+\Theta^+ \to K^-\pi^+K^+n$; this second analysis will be described in more detail in the next section.

Recently the DIANA Collaboration re-analyzed the old K-Xenon bubble-chamber data [9] ($K^+n \to (\bar{K}^0)\Theta^+ \to (\bar{K}^0)\pi^+\pi^-p$) and reported a narrow peak ($\sim$ 10 MeV), located at 1.54 GeV with a statistical significance of 4σ.

The SAPHIR Collaboration reported about the reaction $\gamma p \to \bar{K}^0\Theta^+ \to \pi^+\pi^-K^+(n)$ where a 5σ peak was isolated in the K_S missing mass. The peak was found to be at 1540 ± 5 MeV and a large production cross section of 300 nb was quoted in the paper [12]

Evidence of a narrow structure in the (K_Sp) system was also reported in neutrino and antineutrino collisions with nuclei [13] at CERN. A peak of less than 20 MeV width resonance was found at s mass of 1533 ± 5 MeV with a statistical significance of 6.7σ.

A narrow 4σ peak in the same invariant mass spectrum, located at 1526 ± 3 MeV, was also found by the Hermes Collaboration in the analysis of quasi-real photo production on

a deuteron target. This result, still unpublished, was presented at the above-mentioned Pentaquark Workshop at JLab [14]. A similar result was very recently reported by the ZEUS collaboration [15].

A summary of all these findings is given in Table 1. The results of the CLAS analyses on a proton target, relevant for this proposal, will be discussed in details in the next Section.

Experiment	Reaction	Decay Channel	Mass (MeV)	Width (MeV)	Statistical Significance
Spring-8 [8]	$\gamma n \to K^- \Theta^+$	$K^+ n$	1540	25	4.6 σ
CLAS [10]	$\gamma d \to K^- \Theta^+ p$	$K^+ n$	1542	21	5 σ
Diana [9]	$\gamma Xe \to \Theta^+ X$	$K_s p$	1540	10	4 σ
SAPHIR [12]	$\gamma p \to K^0 \Theta^+$	$K^+ n$	1540	25	5 σ
CERN [13]	$\nu(\bar{\nu}) A \to \Theta^+ X$	$K_s p$	1533	20	6.7 σ
HERMES [14]	$\gamma d \to \Theta^+ X$	$K_s p$	1526	20	4 σ
ZEUS [15]	$e^{+(-)} p \to \Theta^+ X$	$(K_s p) + (K_s \bar{p})$	1527	25	5 σ

Table 1: Recent experimental results for Θ^+ production. The CLAS results on a proton target will be discussed in details in Section 4.

4 Present CLAS measurements

Several photon-induced reactions have been studied by the present authors using the available data on a proton target collected by CLAS in previous years. In the energy range 1.8–3.0 GeV we analyzed the reaction $\gamma p \to \bar{K}^0 \Theta^+$ and subsequent Θ^+ decay to $K^+ n$ or $K^0 p$. At higher energy, 3.0–5.0 GeV, we studied the reactions $\gamma p \to \bar{K}^0 \Theta^+ \to \bar{K}^0 K^+ n$ and $\gamma p \to K^* \Theta^+ \to K^- \pi^+ K^+ n$. In all of these channels we found evidence of a narrow peak in the $(K^+ n)$ invariant mass located in the range 1.55–1.57 GeV. The results of the $\gamma p \to K^* \Theta^+$ channel have been submitted to PRL and are available as a preprint [11]. In the low-energy data set we also observed the presence of a second narrow peak both in the $(K^+ n)$ and $(K^0 p)$ invariant masses located around 1.53 GeV.

4.1 Low-energy analysis

All the available data with photon energy $1.8 < E_\gamma < 3.0$ GeV were analyzed. We studied the two final states:

$\gamma p \to \bar{K}^0 \Theta^+ \to \pi^+ \pi^- K^+ (n)$

$\gamma p \to \bar{K}^0 \Theta^+ \to \pi^+ \pi^- p (K^0)$

The $\bar{K}^0$ (K^0) was identified by detecting its K^0_s component decaying to $\pi^+ \pi^-$ (b.r. $\sim$ 68.6%). For both channels three charged particles in final states were required: $\pi^+ \pi^- K^+$

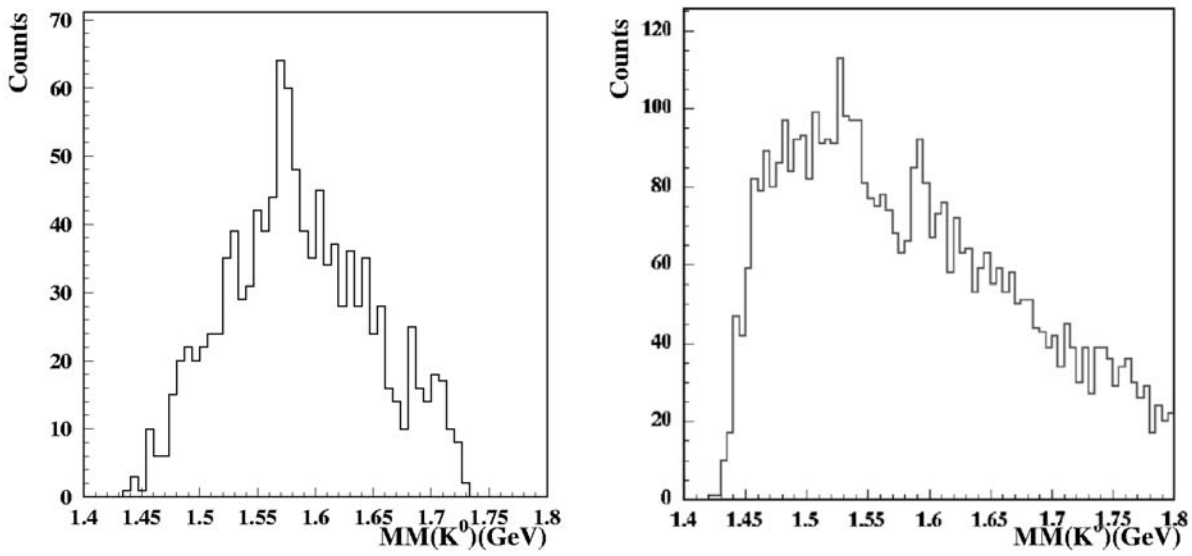

Figure 5: The (K^+n) and (K^0p) invariant masses after all cuts applied.

in the first case and $\pi^+\pi^-p$ in the second case. The neutron (or $K^0/\bar{K}^0$) was identified using the missing mass technique. In the former reaction, the Θ^+ should show up in the $\bar{K}^0$ missing mass while in the latter it should be seen both in the detected K^0 missing mass or in the (K^0p) system invariant mass. We identified as the main sources of physical background the following channels:

- $\gamma p \to K^+\Lambda^*(1520) \to K^+\bar{K}^0 n$,
- $\gamma p \to K^+\Sigma^+\pi^-$,
- $\gamma p \to K^+\Sigma^-\pi^+$

contributing to $\gamma p \to \pi^+\pi^- K^+(n)$, and:

- $\gamma p \to p\phi \to pK_L K_S$,
- $\gamma p \to \Lambda(1110)\pi^+ K^0$

contributing to the other final state. All these channels were efficiently removed by judicious cuts in the analysis. The final (K^+n) and (K^0p) invariant mass spectra showed structures that were enhanced by selecting the low energy region ($1.8 < E_\gamma < 2.3$ GeV), close to the expected production threshold for the Θ^+. The resulting (K^+n) and (K^0p) invariant masses are shown in Fig. 5.

Due to the limited statistics and the large background, the significance of these structures is marginal. Given the experimental conditions of this run (a combination of energy range and magnetic field), full Monte Carlo simulations showed that the maximum detection efficiency for a possible Θ^+ is reached when the $\bar{K}^0$ goes at backward angles in the

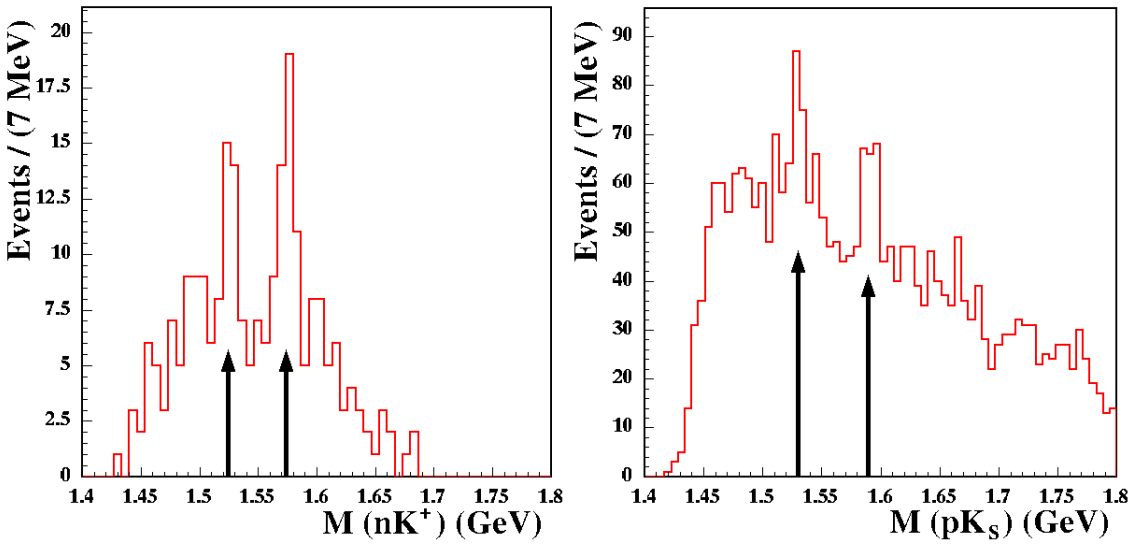

Figure 6: The (K^+n) and (K^0p) invariant masses after selecting K^0 at backward direction ($cos(\theta^{CM}_{K^0}) < -0.35$ in $\gamma p \to \bar{K}^0\Theta^+ \to \pi^+\pi^- K^+(n)$ and $cos(\theta^{CM}_{K^0}) < 0$ for $\gamma p \to \pi^+\pi^- p(K^0)$. The choice of the angular cuts was based on MC simulations of the CLAS acceptance.

center of mass system. Selecting this kinematic region, two narrow peaks show up both in the (K^+n) and (K^0p) invariant masses spectra. The results are shown in Fig. 6. The first peak is located at 1526±5 MeV, with a FWHM∼9 MeV and a statistical significance of 4–6σ (depending on the final state analyzed). The second peak is located at 1572±5 MeV with a similar FWHM and a statistical significance of 6σ. The measured width is compatible with the experimental resolution of CLAS.

Background reactions with known production cross sections, such as $\gamma p \to K^+\Lambda^*(1520) \to K^+K^0n$, $\gamma p \to p\phi \to pK^0_LK^0_S$, and $\gamma p \to p\phi \to pK^+K^-$, were used to infer the integrated luminosity of the data sample. For each of them the yields were corrected by the CLAS detection efficiency evaluated from full Monte Carlo simulations. We estimated an integrated luminosity of:
$\mathrm{L(1.8\text{-}2.3\ GeV})_{g1c} = 2.5\ \mathrm{pb}^{-1}$
From this we were able to derive the total cross section for the peak located around 1570 MeV. The value we found is in the range of $10 - 25$ nb, depending on the reaction mechanism assumed to calculate the efficiency.

Systematic checks of the energy/momentum calibrations were performed to remove possible pion contamination in the kaon sample and to exclude kinematic reflections of meson states in the (K^+n) and (K^0p) invariant mass spectra. However we found no way to account for the two peaks seen in the data.

In conclusion, our preliminary results show a two-peaked structure for the NK spectra. A substantial increase of statistics ($\sim 10\times$) would enable us to determine whether this finding is a statistical anomaly or not, and would also allow us to do extensive systematic

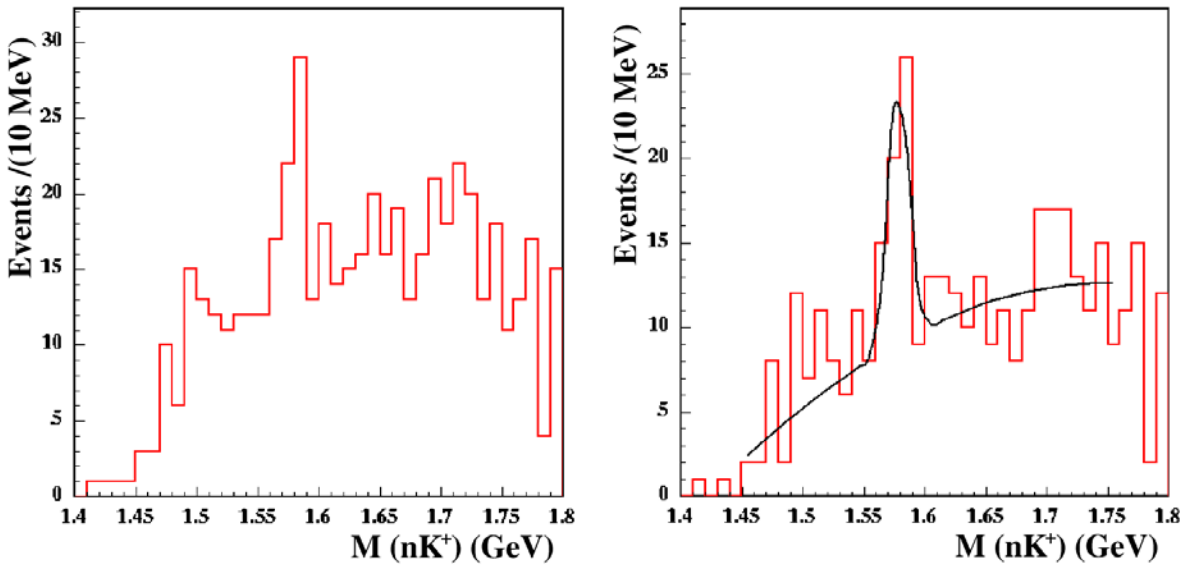

Figure 7: The (K^+n) invariant mass with no angular cuts (left) and after selecting $-0.4 < cos(\theta^{CM}_{K^0}) < 0.5$.

checks.

4.2 High-energy analysis

The available CLAS data with photon energy $3.0 < E_\gamma < 5.0$ GeV were analyzed to search for a Θ^+ signal in the reactions $\gamma p \to \bar{K}^0\Theta^+ \to \bar{K}^0K^+n$ and $\gamma p \to \pi^+K^-\Theta^+$. Possible evidence was found in both channels and will be discussed in more details in the next two sections.

4.2.1 The reaction $\gamma p \to \bar{K}^0K^+(n)$

This reaction was analyzed following the same procedure described in the previous section. The cuts were adapted to the different run conditions (high photon beam energy and high magnetic field) and to the different kinematics. Background reactions were rejected in a similar way. Running Monte Carlo simulations in these kinematics, we found that the maximum detection efficiency was achieved for $\bar{K}^0$ around 90° in the center-of-mass system. Fig. 7 shows the (K^+n) invariant mass without any angular cut and selecting the favored angles. The 6σ peak located at 1578±10 MeV in the (K^+n) invariant mass spectrum has a FWHM∼20 MeV, compatible with the experimental resolution of CLAS in these running conditions [1].

[1]The CLAS experimental resolution at high energy is significantly worse than at low energy because the average momentum of charged particles is higher. This is an important issue to define the best running condition for the proposed experiment. Detailed studies are described in section 5.1.

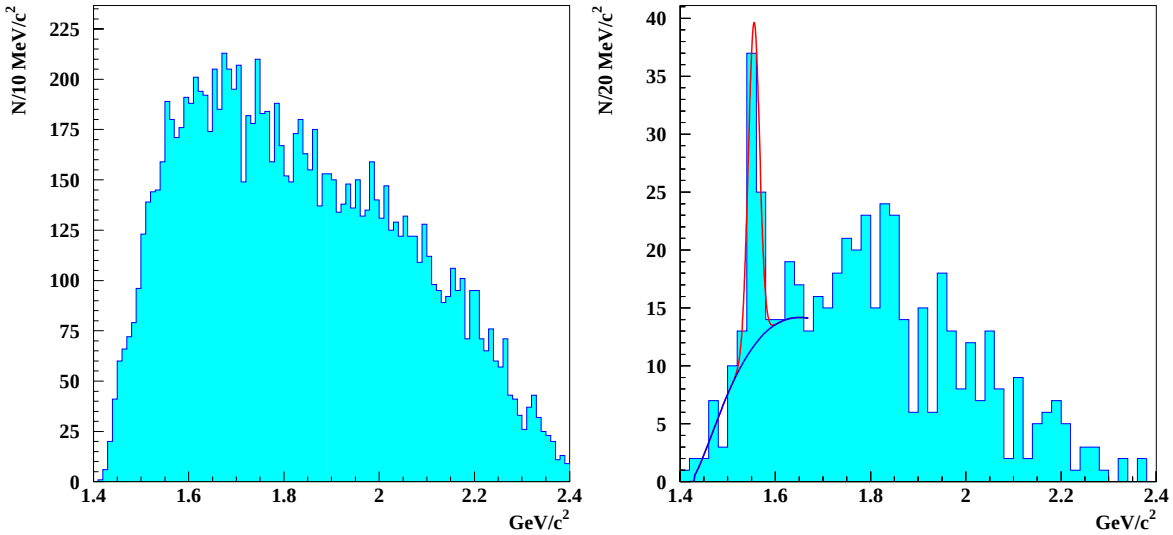

Figure 8: The $M_{(nK^+)}$ invariant mass spectrum in the reaction $\gamma p \to \pi^+ K^- K^+(n)$ integrated over all angles (left) and for $cos\theta^*_{\pi^+} > 0.8$ and $cos\theta^*_{K^+} < 0.6$. The background was estimated from a phase space simulation.

4.2.2 The reaction $\gamma p \to \pi^+ K^- \Theta^+$

The high energy data were also used for the analysis of the reaction $\gamma p \to \pi^+ K^- \Theta^+ \to \pi^+ K^- K^+ n$. More details about the analysis can be found in Ref. [11]. We selected events having a π^+, K^+, and K^- in the final state and identified the channel via the missing mass technique. The main source of background came from ϕ production. which was easily removed by cutting on the (K^+K^-) invariant mass. The left panel in Fig. 8 shows the final (nK^+) invariant mass spectrum. To enhance pion production in the t-channel, two angular cuts in the center-of-mass system were applied. A structure in the region of 1.55 GeV appears after requiring $cos\theta^*_{\pi^+} > 0.8$, where $\theta^*_{\pi^+}$ is the center-of-mass angle between the π^+ and the photon beam. The reaction $\gamma p \to \pi^+ K^- K^+ n$ is dominated by meson production decaying to $K^+K^-\pi^+$ with small momentum transfer to the proton, and baryon resonances decaying to $n\pi^+$ or nK^-. These processes have the K^+ moving forward in the center of mass system. To suppress such backgrounds, an additional cut was applied selecting events having a positive kaon going in the backward direction with $cos\theta^*_K < 0.6$. After these two angular cuts, a peak was clearly observed as shown in the right panel of Fig. 8. The observed mass is M=1555±10 MeV, with FWHM=26±7 MeV and a 7.8 σ statistical significance.

5 Experimental setup and proposed measurement

We propose to measure two production channels on the proton: $K^0\Theta^+$ and $K^*\Theta^+$, each using two decay modes of the Θ^+: K^+n and K^0p, for a total of four final states. The primary goal of the experiment is to establish the mass spectra with a precise measurement of the masses, widths, and errors on any peaks observed. If the two-peak structure is confirmed, we will determine the total and differential cross sections as well as the decay angular distribution.

We propose to use the Hall B Bremsstrahlung tagged photon beam and the CLAS detector with a long hydrogen target. A new longer start counter will be necessary to trigger the experiment. We request an electron beam energy of 4 GeV to obtain tagged photons from the Θ^+ production threshold (1.6 GeV) to the maximum energy of 3.8 GeV. This will allow us to study simultaneously the quoted reactions with a high experimental resolution. We ask for 25 days of beam time with an electron beam current of about 50 nA. This will give us approximately ten times the statistics accumulated in the present preliminary analysis of the low-energy data. Experiments with similar requirements have successfully run in Hall B (g6a-b-c). With these statistics we can rule out statistical anomalies and will have enough data to perform a number of systematic checks on the experiment.

5.1 Kinematics and Monte Carlo simulations: choice of magnetic field and energy range

The choice of a hydrogen target is set by the need for a complete determination of the production channels and decay modes of the Θ^+. However, experimentally we must optimize the beam energy, trigger setup and values of CLAS toroidal field. These issues have been addressed by performing full MC simulations and exploiting the experience gained analyzing the existing data.

Monte Carlo events were generated with a theoretical model for the production of the $K^0\Theta^+$ final state. The response of the CLAS detector to the final-state particles was determined by the GSIM package. We did runs for four different values of the B-field to optimize the settings. In general, we expect the efficiency to detect all of the final-state particles to drop with increasing B-field, because of loss of inbending particles at high values of the B-field. In contrast, the invariant-mass and missing-mass resolutions should get better with increasing B-field. Since the statistical significance of any observed peak goes roughly as $S/\sqrt{B}$ where S is the signal and B is the background yield, and since S and B are proportional respectively to efficiency and efficiency$\times$resolution, we might expect the statistical significance of the peaks to go as the $\sqrt{efficiency/resolution}$. Thus we want to maximize the ratio of efficiency to resolution. The expected efficiencies and resolutions are plotted versus photon energy for different values of B-field in Figs. 9, 10, and 11. Above a photon energy of 3 GeV, the efficiency drops by about 30% as the B-field increases from 50% to 88% of full value. At lower energies, the drop-off is more extreme. If lower energies dominate the cross-section, as model calculations indicate, then it is

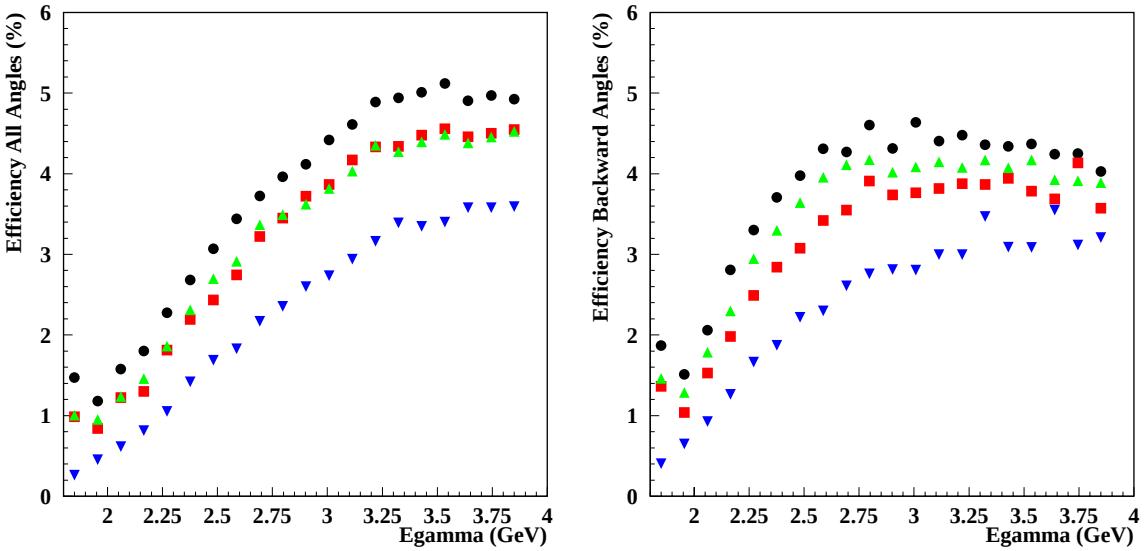

Figure 9: Detection efficiency for all angles (left) and at backward angles (right) as a function of the photon energy with four field settings: black-dots=50%; red-squares=58%, green-triangles=65% and blue-reverse-triangles=88%.

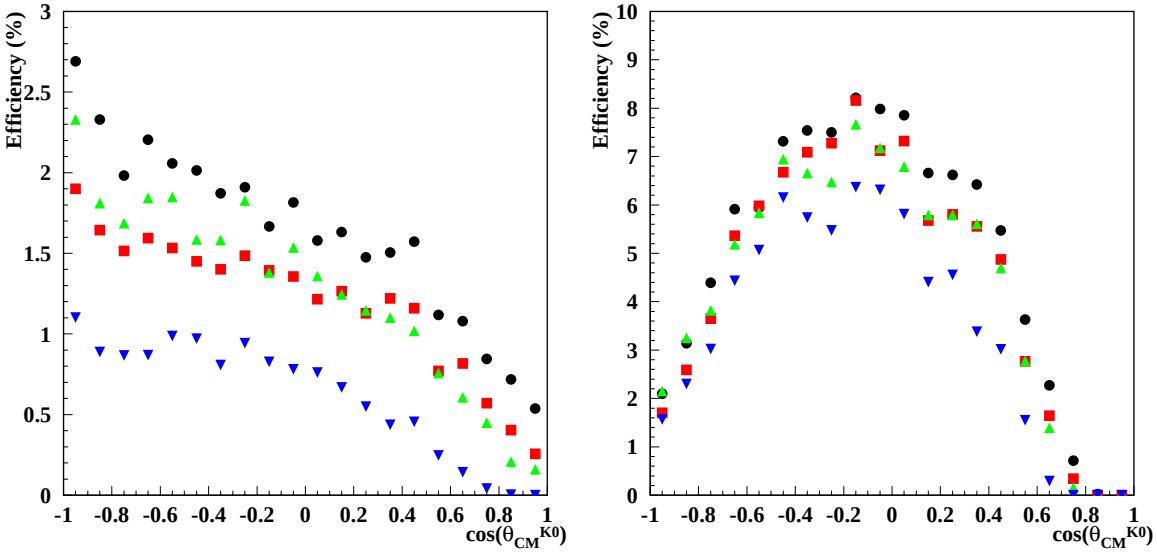

Figure 10: Detection efficiency as a function of the K^0_{CM} angle for 1.8< E_γ <2.3 GeV (left) and 3.3< E_γ <3.8 GeV (right) with four field settings: black-dots=50%; red-squares=58%, green-triangles=65% and blue-reverse-triangles=88%.

Reaction	Θ^+ Mass resolution (MeV)	Detection efficiency (%)
$\gamma p \to \bar{K^0}\Theta^+ \to \pi^+\pi^- K^+(n)$	4-18	1.5-5
$\gamma p \to K^0\Theta^+ \to \pi^+\pi^- p(K^0)$	5-18	3-14
$\gamma p \to \bar{K^*}\Theta^+ \to \pi^+ K^+ K^-(n)$	5-15	$\sim$0.1

Table 2: Estimated mass resolution and efficiency. The indicated range corresponds to the photon energy range from Θ^+ threshold to 4 GeV.

important to run at lower B-field. The expected drop in resolution is much smaller, because the missing-mass resolution is not dominated by measurement errors in the tracking chambers. At these particle energies, multiple scattering and angle measurement errors still play a large role. For these reasons, we expect to run at 50% of full field.

The beam energy decision is obviously impacted strongly by our estimates of the energy dependence of the cross-section. Model calculations indicate a fast fall-off with energy. On the other hand, the efficiency for detecting the full final state increases up to a photon energy of 3 GeV. To cover this photon energy range, we choose to run with an electron beam energy of 4 GeV.

Table 2 summarizes the mass resolution and efficiency obtained from MC simulations of various final states with chosen magnetic field and beam energy configuration.

5.2 New Start Counter

The existing Start Counter [37] is 40 cm long and can not be operated with a 40 cm target cell. It has to be replaced with a new one. The requirements for the new Start Counter are the following:

- It must be able to deal with the high rate induced by the e.m. background from the target;
- It must have a time resolution comparable to, or better, than the existing one;
- It must be segmented, at least, in six sectors in ϕ angle (one per each sector of CLAS) to allow time and geometric coincidence with CLAS and the tagger at the trigger level.

The design of this new device is in progress. The expected time resolution will be of the order of a few ns, allowing for a coincidence with the tagger and the CLAS in a 10-15 ns window. In the following, we assume a new Start Counter fulfilling these minimum

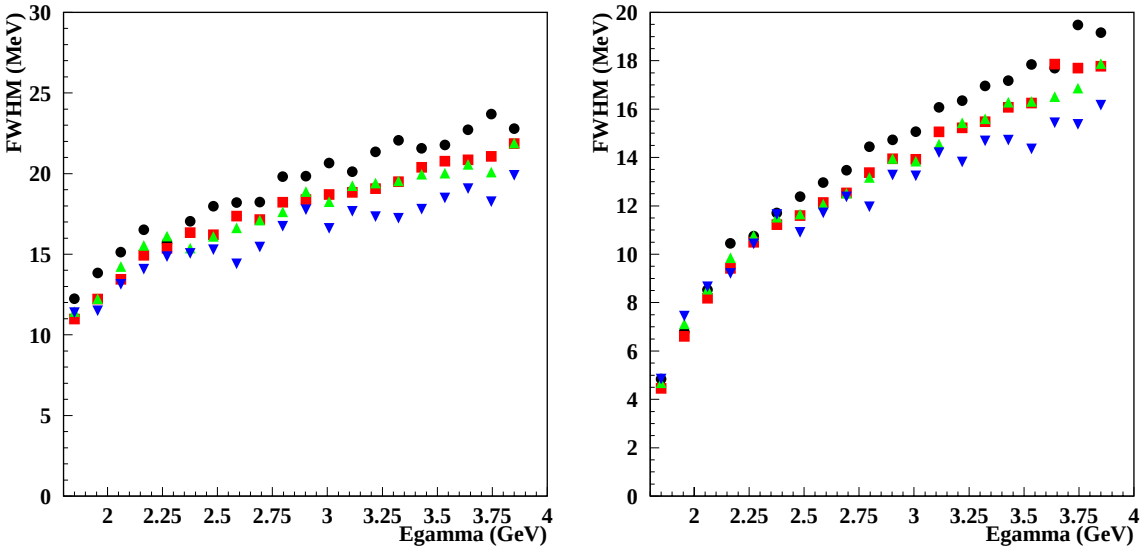

Figure 11: Expected resolution for the neutron missing mass (left) and Θ^+ mass (right) in the reaction $\gamma p \to \bar{K}^0\Theta^+ \to \pi^+\pi^- K^+(n)$ as a function of the photon energy with four field settings: black-dots=50%; red-squares=58%, green-triangles=65% and blue-reverse-triangles=88%.

requirements. Extrapolating the existing Start Counter rates from previous runs, where the same electron beam current was used on an 18 cm long target, we expect a single PMT rate of about 1.2 MHz, which is within the optimal operating condition. In the off-line analysis, the high number of charged particles recorded in each event will constrain the start time, allowing a tight coincidence ($\sim$ 1ns) with the tagger, and rejecting most of the random hits and noise.

5.3 Running conditions

As already mentioned, one of the goals of this experiment is to confirm the existence of the two peaks observed in the analysis of the low-energy data. Thus, we will optimize the trigger and calculate the expected rates by extrapolating the experimental conditions of that run. The average electron beam current was 10–12 nA and the electron beam energy was varied from 2.4 to 3.1 GeV. The Bremsstrahlung photon beam was produced with a gold radiator having a thickness of 10^{-4} radiation lengths. The target was an 18 cm long cell filled with liquid hydrogen, ρ=0.071g/cm^3. From the analysis of those data we observed a total of 16 $\Theta^+(1526)$ and 30 $\Theta^+(1571)$ candidates as shown in Fig. 6 for an integrated luminosity (1.8$<E_\gamma<$2.3 GeV) estimated to be $\sim$ 2.5 pb^{-1}.

To obtain 10$\times$ more statistics in the same energy range and extend the measurement to the $\bar{K}^*\Theta^+$ channel we will run with a 4 GeV electron beam impinging on the 10^{-4} radiation lengths radiator, and with a 40 cm long hydrogen target. The electron beam current will be 50 nA providing a photon flux of $\phi_\gamma \sim 6.7 \cdot 10^6$ γ/s in the energy range from 1.6 to 2.3 GeV. Such a flux will allow us to obtain in 25 days of data taking an integrated luminosity of

$$L(1.8 < E_\gamma < 2.3) = \phi_\gamma T_{length} \rho \mathcal{N}_A \cdot time = 25\, pb^{-1}.$$

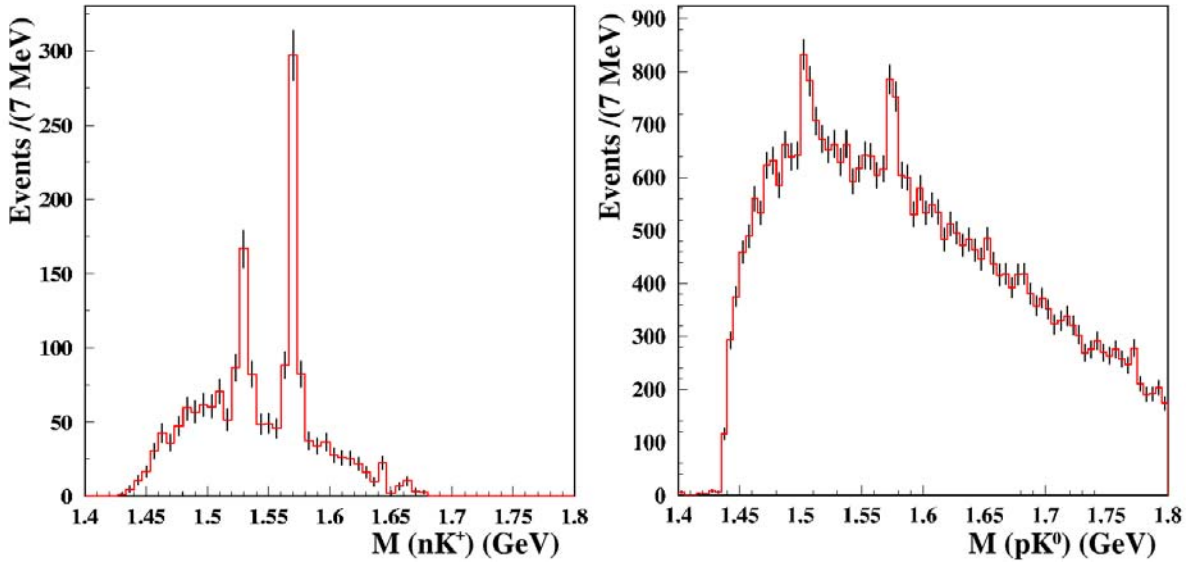

Figure 12: The (K^+n) (left) and pK^0 (right) invariant mass spectra for K^0 at backward angles in the center-of-mass system.

The entire CLAS tagger will be read out during data taking, covering from 20% to 95% of the electron beam energy, i.e. 0.8-3.8 GeV. Only the upper portion of the tagger will trigger the data acquisition, together with CLAS and the Start Counter, in order to select photon energies above the Θ^+ threshold (1.6 GeV). Since we are interested in final states with three charged particle we will require the detection of at least two charged particles in CLAS. The final estimated rate is

$$R_{trigger} = 4.1\ kHz$$

which is within the DAQ limits. This includes 50% of hadronic events above the Θ^+ threshold and 50% of accidental coincidences. The accidental rate will be reduced by a factor of ten in the off-line analysis by requiring tight timing coincidences between the different components of the apparatus. More details about rate estimates are given in the Appendix.

5.4 Statistical accuracy

By extrapolating the results obtained from the low-energy data analysis, we can estimate the statistical accuracy of the proposed experiment. As discussed in section 4, the two peaks were better seen in the energy range $E_\gamma = 1.8 - 2.3$ GeV. The projected yields reported below refer to this energy range and therefore represent a lower limit of the achievable statistics. Detailed results are shown for the reactions $\gamma p \to \bar{K}^0\Theta^+ \to \pi^+\pi^- K^+(n)$ and $\gamma p \to \bar{K}^0\Theta^+ \to \pi^+\pi^- p(K^0)$.

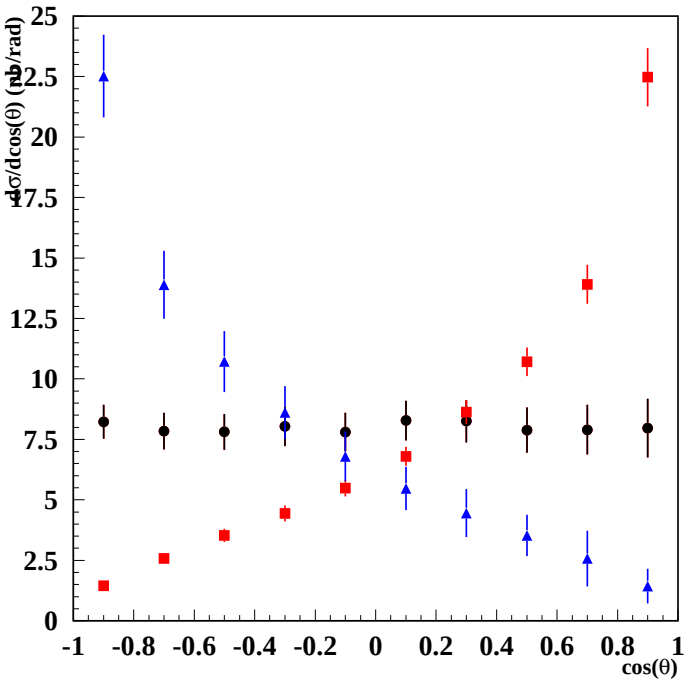

Figure 13: The expected errors on the differential cross section according to different production mechanisms: flat (black-dots), u-channel production (blue-triangles), and t-channel (red-squares).

We assumed a 50% torus field configuration, a production cross section of 16 nb, equal branching ratios for Θ^+ decaying to nK^+ and pK^0, and an integrated luminosity corresponding to 25 days/run. According to the previous analysis, we expect 160(700) $\Theta^+(1526)$ and 300(500) $\Theta^+(1571)$ candidates for the nK^+ (pK^0) final state, cutting at backward angles. The expected nK^+ and pK^0 invariant mass spectra (corresponding to Fig. 6) are shown in Fig. 12. With the same assumptions, the expected statistical error on the differential cross section has been estimated. Fig. 13 shows the expected results for the $\gamma p \to \bar{K}^0\Theta^+ \to \pi^+\pi^- K^+(n)$ channel, according to different hypotheses on production mechanism: a flat distribution in the $(K^0 - \Theta^+)$ center-of-mass, u-channel production, and t-channel production. In this energy range ($E_\gamma = 1.8 - 2.3$), we expect to measure the whole angular distribution (see also Fig. 9). With the chosen binning, the expected relative statistical error is around 10%, sufficient to disentangle the different production mechanisms. Similar results are expected also for the $\gamma p \to \bar{K}^*\Theta^+$ reaction.

5.5 Systematic errors

With a data sample ten times larger than the present one, we will be able to do a number of systematic checks of the consistency of the results that will address the following:

- check the presence of kinematical reflections that could distort or produce peaks in the mass spectra;
- vary the analysis by testing tighter and looser cuts;

- check the consistency of results obtained from different decay modes;
- check kinematical correlations of different masses by constructing Dalitz plots;
- compare equivalent areas of detector as, for example, yields from different CLAS sectors.

Clearly, such extensive study is not within reach with the presently available statistics.

6 Summary

Experimental evidence for a pentaquark state of baryonic matter is increasingly convincing. However, many small contradictions plague the comparison of experimental results. No single experiment has the statistical power to rule out the chance of a correlation between a statistical fluctuation and an unknown systematic enhancement acting to produce the state. The previous PAC approved the running of the "g2c" experiment to corroborate the observation of the Θ^+ in the final state of $pK^+K^-(n)$ produced by photoproduction on deuterium. To complete our experimental goal of firmly establishing the phenomenology of the Θ^+ spectrum, we propose a similar measurement for photoproduction of Θ^+K^0 and Θ^+K^* from a proton target. With ten times the statistics of our present data sample, this new experiment will enable us to pin down the masses and widths of any peaks in the spectrum, including the assignment of systematic as well as statistical errors to the mass and width values. As a secondary goal, if the "two-peak" nature of the spectrum is confirmed, we will be able to measure the differential cross section as well as the total cross section helping to determine the relevance of pentaquark production mechanisms.

A Appendix: Rate estimates

A.1 Tagger rate

The entire CLAS tagger will be read out during data taking, covering from 20% to 95% of the electron beam energy, i.e. 0.8–3.8 GeV. The rate of the entire tagger will be 46 MHz. This corresponds to a rate of 140 kHz on each E-counter and 860 kHz on each T-counter [35]. Only the upper 40 T-counters will be used for triggering, selecting photon energy greater than 1.6 GeV, which is close to the presently estimated Θ^+ threshold. The corresponding rate (Master OR) going to the trigger logic will be 24 MHz. Due to the high photon flux, the probability of multiple hits in the tagger is not negligible. This can be estimated as

$$R_{tagger}^{multiple\ hits} = 2 \times \Delta\tau\phi_\gamma(1.6-3.8) \times \phi_\gamma(0.8-3.8) = 2.2 \cdot 10^6 s^{-1},$$

where the time coincidence of $\Delta\tau = 1$ ns reflects the time resolution achievable in the off-line analysis. This rate corresponds to 9% of the MOR rate. Most of these events will be recoverable in the final analysis since typically one of the two photons will have an energy which is not compatible with the total energy observed in the detector.

A.2 CLAS, Start Counter, and Trigger Rates

Since we are interested in final states with three charged particles, we will require at trigger level the detection of at least two charged particles in CLAS. The relevant hadronic rate comes from photons (mainly untagged) above the two pion threshold: $\phi_\gamma(> 2\pi) = 6.9 \cdot 10^7$ γ/s.

$$R_{hadron} = \phi_\gamma(> 2\pi) T_{length} \rho \mathcal{N} \sigma_{hadron} = 12kHz$$

assuming a photo-absorption cross section of $\sigma_{hadron} = 100$ μbarn. Approximately 35% of these events comes from photons with energy above 1.6 GeV which are relevant for this proposal ($R_{hadr}^{\text{“}true''} = 4.1$ kHz), 35% from tagged photon between 0.8 and 1.6 GeV, and 30% from untagged photons. All these events will produce hits in the Start Counter, which has almost 100% acceptance, while CLAS will see only a portion of them.

In addition to hadronic events, the Start Counter will also be affected by the electromagnetic background produced by the photon beam, mainly Compton scattering and pair production. Following Ref. [36] and extrapolating the rates of previous CLAS experiments, in this experiment the electromagnetic background is estimated to produce a total rate of 8.9 MHz, dominated by single hits. Most of this background will be removed by requiring the coincidence of two or more hits in the Start Counter. The segmentation of the new device will allow us to achieve reasonable rates with no loss of good events. Using a 10 ns time coincidence, the final rate is expected to be reduced to

$$R_{ST}^{BG} = 1\ MHz.$$

This has to be compared with the total hadronic rate which, as mentioned in the previous section, is expected to be

$$R_{ST}^{Hadr} = 12\ kHz$$

The DAQ will be triggered by a coincidence of CLAS, Start Counter, and MOR. The final estimated rate is

$$R_{trigger} = 4.1\ kHz$$

which is within the DAQ limits. This includes random coincidences, and the CLAS acceptance for two hadrons, as discussed in the next section.

A.3 Trigger Logic and Accidental Rates

To select photons with energy above 1.6 GeV, the MOR will be used in coincidence with the Start Counter within a 10 ns coincidence window. The $MOR \times ST$ coincidence rate will be affected by two type of accidentals:

1) Hadronic events in the Start Counter induced by photons which are below the minimum triggered energy of 1.6 GeV;

2) Hits in the Start Counter induced by the electromagnetic background.

Assuming a coincidence window of 10 ns, we have:

$$\begin{aligned} R_{MOR\times ST}^{acc_1} &= 2 \cdot \Delta\tau \cdot \phi_\gamma(tagged) \cdot (R_{ST}^{Hadr} - R_{ST}^{Hadr}(tagged)) = 3.7kHz \\ R_{MOR\times ST}^{acc_2} &= 2 \cdot \Delta\tau \cdot \phi_\gamma(tagged) \cdot R_{ST}^{BG} = 510kHz. \end{aligned}$$

After requiring the coincidence with CLAS, the first accidental rate will be reduced by the CLAS acceptance for the detection of two charged particles, $\epsilon_{CLAS} \sim 50\%$, since the hadronic event causing the signal in the Start Counter can also give a signal in CLAS. On the contrary, the second rate will be reduced to a much grater extent, since it is uncorrelated with CLAS. The final accidental rates are estimated to be:

$$\begin{aligned} R_{(MOR\times ST)\times CLAS}^{acc_1} &= R_{MOR\times ST}^{acc_1} \times \epsilon_{CLAS} = 1.8\ kHz \\ R_{(MOR\times ST)\times CLAS}^{acc_2} &= 2 \cdot \Delta\tau \cdot R_{MOR\times ST}^{acc_2} \cdot (R_{ST}^{Hadr} - R_{ST}^{Hadr}(tagged)) \times \epsilon_{CLAS} = 200Hz. \end{aligned}$$

In this case the coincidence window is $\Delta\tau = 100$ ns. The total DAQ rate is then:

$$R_{trigger} = R_{hadr}^{\text{“}true''} \times \epsilon_{CLAS} + R_{(MOR\times ST)\times CLAS}^{acc_1} + R_{(MOR\times ST)\times CLAS}^{acc_2} = 4.1\ kHz$$

In the off-line data analysis the “true” events will be extracted from the total recorded events using a tighter time coincidence between Start Counter and MOR. Previous analyses have shown that the time resolution achievable in multi-particle events is of the order of 200 ps, allowing us to use a 1 ns time window. This will reduce the accidental rates to respectively 180 and 20 Hz. The former can be further suppressed because in most of the cases the real photon which caused the hadronic event will also be recorded in the tagger. The final contamination to the true rate due to accidentals is therefore estimated to be less than 10%.

A.4 Trigger Efficiency

The trigger rate for this experiment strongly depends on the CLAS acceptance for the detection of multiparticle final states.

As described above, to reduce the total hadronic rate we need to require at least two charged particles in CLAS. This is accomplished by using the CLAS Level 2 Trigger electronics. This is capable of detecting the presence of at least one track in a CLAS sector with no information on the multiplicity. Thus, the trigger will require the presence of tracks in at least two CLAS sectors.

The trigger effect was studied both in relation to the hadronic rates reduction and to the loss of efficiency for the Θ^+ channels. For this purpose we performed full Monte Carlo simulations of the dominant multiparticle final states in the photoabsorption process and of our channels. These indicate that the trigger causes a reduction of the hadronic event rate in CLAS of $\epsilon_{CLAS} \sim 50\%$, This value was also confirmed by the analysis of previous CLAS run which used a single particle trigger. On the contrary, no significant bias was found in the reactions involving the Θ^+. In fact, simulations indicate that almost 100% of the reconstructed events had hits in at least two different CLAS sectors.

References

[1] Particle Data Book, 1986.

[2] H.J. Lipkin, in 'Hadrons, Quarks and Gluons', Proceedings of the Hadronic Session of the XXIInd Rencontre de Moriond, Edited by J. Tran Thanh Van, Editions Frontières, Gif Sur Yvette - France (1987), p.691;
H.J. Lipkin, Nucl. Phys. A **625**, 207 (1997).

[3] H. Högaasen and P. Sorba, Nucl. Phys. B **145**, 119 (1978);
M. de Crombrugghe, H. Högaasen and P. Sorba, Nucl. Phys. B **156**, 347 (1979).

[4] A.V. Manohar, Nucl. Phys. B **248**, 19 (1984).

[5] M. Chemtob, Nucl. Phys. B **256**, 600 (1985).

[6] M. Praszalowicz, in Skyrmions and Anomalies (M. Jezabek and M. Praszalowicz, eds.), World Scientific (1987), 112-131;
M. Praszalowicz, Phys. Lett. B **575**, 234 (2003).

[7] D. Diakonov, V. Petrov and M. Polyakov, Z. Phys. A **359**, 305 (1997).

[8] T. Nakano et al., Phys. Rev. Lett. **91**, 012002 (2003).

[9] V.V. Barmin et al., Phys. Atom. Nucl. **66**, 1715 (2003); Yad. Fiz. **66**, 1763 (2003).

[10] S. Stepanyan et al., hep-ex/0307018, accepted by PRL.

[11] V. Kubarovsky et al., hep-ex/0311046.

[12] J. Barth et al., Phys. Lett. B **572**, 127 (2003).

[13] A.E. Asratyan, A.G. Dolgolenko, and M.A. Kubantsev, preprint hep-ex/0309042, submitted to Yad. Fis.

[14] Unpublished, see for example the presentation at the Penta-Quark 2003 Workshop, Jefferson Lab, November 6-8, 2003:
http://www.jlab.org/intralab/calendar/archive03/pentaquark/talks/lorenzon.pdf.

[15] Unpublished, see *http://webcast.desy.de/DESY_Forum_251103.htm.*

[16] C. Alt et al., hep-ex/0310014.

[17] Pentawork Workshop, Jefferson Lab, November 6-8, 2003.

[18] R. Jaffe and F. Wilczek, hep-ph/0307341.

[19] M. Karliner and H.J. Lipkin, Phys. Lett. B **575**, 249 (2003).

[20] S. Capstick, P.R. Page and W. Roberts, Phys. Lett. B **570**, 185 (2003); P.R. Page, hep-ph/0310200.

[21] F. Csikor, Z. Fodor, S.D. Katz and T.G. Kovács, hep-lat/0309090; S. Sasaki, hep-lat/0310014.

[22] Shin-Lin Zhu, hep-ph/0307345; J. Sugiyama, T. Doi and M. Oka, hep-ph/0309271.

[23] F. Close, hep-ph/0311087.

[24] D. Borisyuk, M. Faber and A. Kobushkin, hep-ph/0307370.

[25] B.K. Jennings and K. Maltman, hep-ph/0308286.

[26] R. Bijker, M. M. Giannini and E. Santopinto, hep-ph/0310281.

[27] W. Liu and C.M. Ko, e-Print Archive: nucl-th/0‘308034.

[28] W. Liu and C.M. Ko, e-Print Archive: nucl-th/0309023.

[29] S.I. Nam al., e-Print Archive: hep-ph/0308313.

[30] Y. Oh et al., e-Print Archive: hep-ph/0310019.

[31] M. Guidal, M, Vanderhaeghen, and M. Polyakov, private comunication.

[32] M. Polyakov, private communication, 2003.

[33] W. Liu, C.M. Ko,V. Kubarovsky, in preparation.

[34] R. Arndt et al., Phys. Rev. C **68**, 042201 (2003).

[35] D. I. Sober *et al.*, Nucl. Instrum. Meth. A **440**, 263 (2000).

[36] M. Guidal, C. Marchan, and E. Smith, *Electromagnetic Background in the Start Counter Induced by Photons*, CLAS-note 95-009.

[37] S. Taylor *et al.*, Nucl. Instrum. Meth. A **462**, 484 (2001).